

Subtidal storm-influenced carbonate ramp model : Galena Group (Middle Ordovician) along Mississippi River (Iowa, Wisconsin, Illinois and Missouri), USA

Autor(en): **Bakush, Sadeg H. / Carozzi, Albert V.**

Objektyp: **Article**

Zeitschrift: **Archives des sciences et compte rendu des séances de la Société**

Band (Jahr): **39 (1986)**

Heft 2: **Archives de Sciences**

PDF erstellt am: **22.07.2024**

Persistenter Link: <https://doi.org/10.5169/seals-740356>

Nutzungsbedingungen

Die ETH-Bibliothek ist Anbieterin der digitalisierten Zeitschriften. Sie besitzt keine Urheberrechte an den Inhalten der Zeitschriften. Die Rechte liegen in der Regel bei den Herausgebern. Die auf der Plattform e-periodica veröffentlichten Dokumente stehen für nicht-kommerzielle Zwecke in Lehre und Forschung sowie für die private Nutzung frei zur Verfügung. Einzelne Dateien oder Ausdrucke aus diesem Angebot können zusammen mit diesen Nutzungsbedingungen und den korrekten Herkunftsbezeichnungen weitergegeben werden. Das Veröffentlichen von Bildern in Print- und Online-Publikationen ist nur mit vorheriger Genehmigung der Rechteinhaber erlaubt. Die systematische Speicherung von Teilen des elektronischen Angebots auf anderen Servern bedarf ebenfalls des schriftlichen Einverständnisses der Rechteinhaber.

Haftungsausschluss

Alle Angaben erfolgen ohne Gewähr für Vollständigkeit oder Richtigkeit. Es wird keine Haftung übernommen für Schäden durch die Verwendung von Informationen aus diesem Online-Angebot oder durch das Fehlen von Informationen. Dies gilt auch für Inhalte Dritter, die über dieses Angebot zugänglich sind.

**SUBTIDAL STORM-INFLUENCED CARBONATE RAMP MODEL:
GALENA GROUP (MIDDLE ORDOVICIAN)
ALONG MISSISSIPPI RIVER (IOWA, WISCONSIN, ILLINOIS
AND MISSOURI), U.S.A.**

BY

Sadeg H. BAKUSH and Albert V. CAROZZI ¹

ABSTRACT

The Galena Group (Middle Ordovician) along the Mississippi River was studied by means of six field sections and four cores. Detailed petrographic study of 1773 oriented thin sections led to the recognition of seven distinct carbonate microfacies, among which five represent fair-weather conditions and two storm events. The vertical succession and correlation coefficients of the microfacies permitted the recognition of an ideal shallowing-upward sequence which in turn was converted into a horizontal depositional model.

The depositional model consists of a shallow open marine subtidal carbonate ramp with the following fair-weather environments and their microfacies (1, 2, 3, 4 and 7) from offshore to onshore: slope (calcsiltite with up to 10% scattered sand-size bioclasts); outer platform (mud- to grain-supported brachiopod-pelecypod bioaccumulated limestone with calcsiltite matrix, mud-supported biocalcarenite with pelletoidal calcsiltite matrix and grain-supported biocalcarenite with pelletoidal calcsiltite matrix and rare sparite cement); and shoal (grain-supported to pressure-welded crinoidal-brachiopod-bryozoan calcarenite with sparite cement). The model lacks the more shallow environments because the Galena sea covered most of the North American continent and the shoreline was far from the investigated area.

The storm events display their maximum intensity in the shallower portion of the outer platform where they are represented by microfacies 5, a coarse disorganized grain-supported biocalcirudite with sparite cement and rare pelletoidal calcsiltite matrix. As the storms decrease in intensity landward and over the shoal, microfacies 6 was deposited, a less disorganized grain-supported and graded bedded biocalcarenite with sparite cement and rare calcsiltite matrix. The Galena Group consists of twenty-five symmetric and asymmetric cycles divided into at least five successive predominant storm- and fair-weather episodes.

The diagenetic features observed petrographically represent changes that took place in the following environments: marine phreatic; undersaturated freshwater phreatic I; saturated freshwater phreatic I; mixed marine freshwater phreatic with intense Dorag dolomitization; tectonic uplifting of the dolomites; undersaturated freshwater phreatic II (dedolomitization); saturated freshwater phreatic II; burial, and Mississippi Valley type mineralization.

¹ Department of Geology, University of Illinois at Urbana-Champaign, Urbana, Illinois, 61801, U.S.A. This paper is part of a doctoral dissertation completed by S. H. B. under the supervision of A. V. C. and submitted to the Graduate College in May 1985.

This research was entirely supported by El Fateh University in Tripoli, Socialist People's Libyan Arab Jamahiriya and the People's Committee for Students of the S.P.L.A.J. which also defrayed part of the publication costs. The State Geological Surveys of Illinois and Iowa, and the Missouri Department of Natural Resources are thanked for generously providing the core samples.

RÉSUMÉ

Le Groupe Galena (Ordovicien moyen) le long du Mississippi a été étudié au moyen de six coupes stratigraphiques à l'affleurement et de quatre sondages entièrement carottés. L'étude pétrographique détaillée de 1773 coupes minces orientées a révélé l'existence de sept microfaciès carbonatés, parmi lesquels cinq représentent des conditions de sédimentation de beau temps et deux des conditions de tempêtes. La succession verticale des microfaciès et leurs coefficients de corrélation ont permis de reconstruire une série idéale de profondeur décroissante vers le haut qui à son tour a été transformée en un modèle dépositionnel.

Le modèle dépositionnel correspond à une rampe carbonatée subtidale de mer ouverte avec ses milieux de beau temps et leurs microfaciès (1, 2, 3, 4, et 7) qui sont les suivants en direction de la côte: pente (calcsiltite avec jusqu'à 10% de bioclastes); plateforme externe (calcaire bioaccumulé à brachiopodes et pélicypodes et matrice de calcsiltite, biocalcarenite à grains non jointifs et à matrice de calcsiltite pelletoidale, biocalcarenite à grains jointifs avec matrice de calcsiltite pelletoidale et rare ciment sparitique); haut-fond (calcarenite à crinoïdes-brachiopodes-bryozoaires à grains jointifs et ciment sparitique). Les milieux les moins profonds manquent dans ce modèle car la mer de Galena couvrait la plus grande partie du continent nord-américain et la ligne côtière était très éloignée de la zone étudiée.

Les tempêtes montrent leur maximum d'intensité dans la partie la moins profonde de la plateforme externe où elles sont représentées par le microfaciès 5, une biocalcirudite grossière et désorganisée à grains jointifs et à ciment sparitique. Avec la diminution de l'intensité des tempêtes en direction de la côte et au-dessus du haut-fond, une biocalcarenite moins désorganisée, à grains jointifs et à granulométrie décroissante vers le haut a été déposée (microfaciès 6). Le Groupe Galena comprend 25 cycles symétriques et asymétriques qui peuvent se subdiviser au moins en cinq épisodes de beau temps et de tempêtes.

Les caractéristiques diagénétiques observées sous le microscope représentent les changements qui ont eu lieu dans les milieux suivants: marin phréatique, eau douce phréatique sous-saturé I, eau douce phréatique saturé I, mélange phréatique d'eau salée et d'eau douce avec dolomitisation intense de type Dorag, soulèvement tectonique des dolomies, eau douce phréatique sous-saturé II (dédolomitisation), eau douce phréatique saturé II, enfouissement avec minéralisation de type Mississippi Valley.

INTRODUCTION

The present study is based on detailed sampling of field sections and cores of the Galena Group (Middle Ordovician) along the Mississippi River in northern Iowa, SW Wisconsin, northern Illinois, SE Iowa, SW Illinois and NE and SE Missouri. Its main purpose is to investigate depositional-diagenetic environments of the Galena Group in the study area by determining the temporal and spatial distribution of its various microfaciès.

STRATIGRAPHY AND PREVIOUS WORK

The stratigraphic basis (Figure 1) for this petrographic study of the Galena Group consists of the formations and members proposed by Templeton and Willman (1963) and Willman and Kolata (1978). A detailed account of the numerous previous biostratigraphic and petrographic works is given by Bakush (1985). However, a few of the most recent ones are of particular interest to this study. Delgado (1980 and 1983)

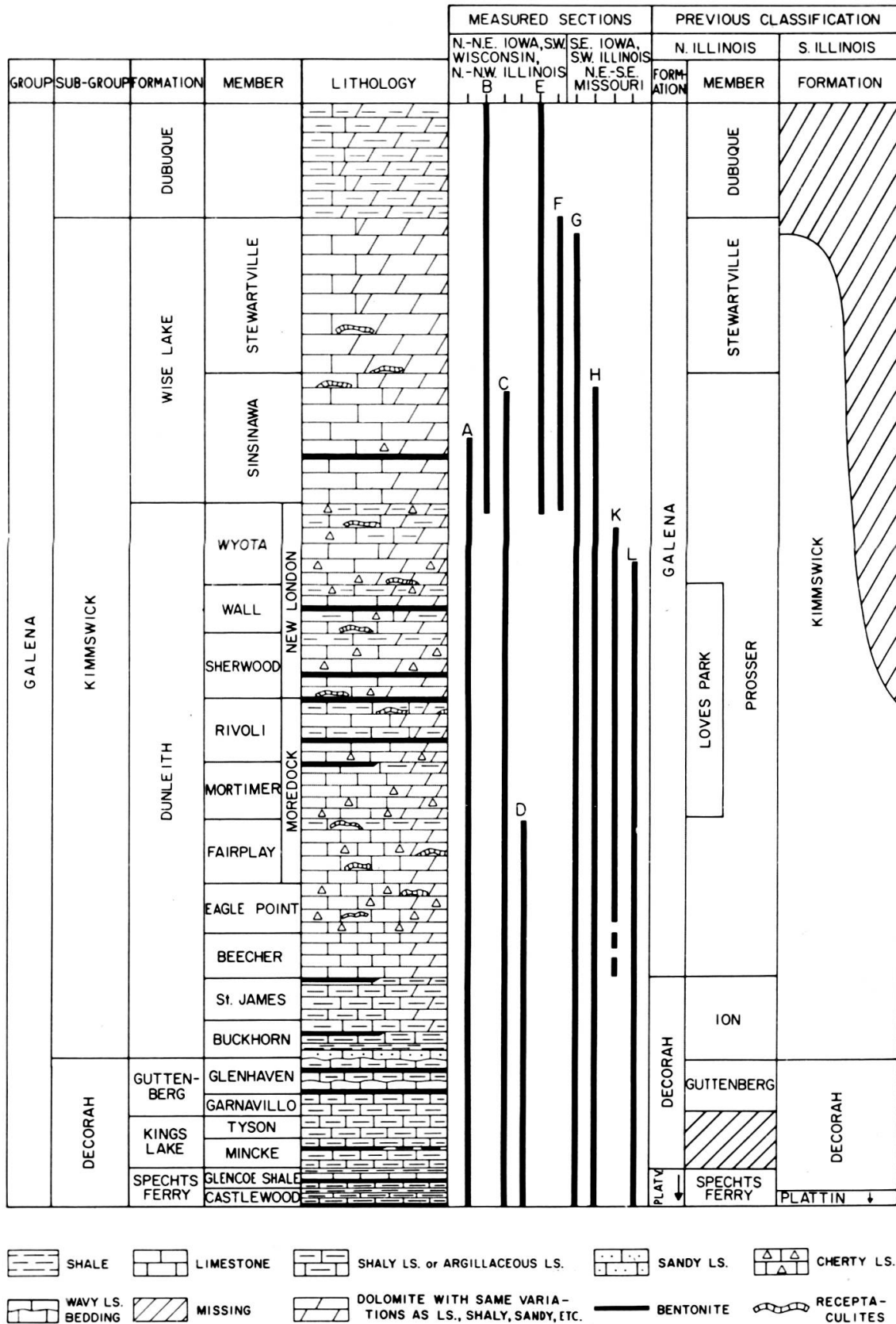


FIG. 1.

Columnar section of Galena Group (modified from Templeton and Willman, 1963).

concluded that the Galena Group in the Upper Mississippi Valley was deposited in a calm subtidal environment on a highly stable uniform marine shelf, below normal wave base and generally within the photic zone. Delgado (1983) identified a minimum of 153 separate hardground surfaces in the Dunleith, Wise Lake and Dubuque Formations representing a spectacular display of submarine cementation. He estimated the total hiatus corresponding to hardgrounds to be about 15 to 30% of Galena deposition time.

Delgado (1983) was the first to report storm deposits in the Galena Group based on the occurrence of thin (1-13 cm) bioclastic grainstone beds with sharp scoured basal surfaces and gradational upper boundaries. He stated that the grainstone beds may show graded bedding, imbrication, cross-bedding, hummocky cross-stratification, or parallel lamination. He described molluscan shells in these beds as disarticulated or broken and large intraclasts generally not highly abraded. Several beds of K-bentonite occur in the Galena Group and represent submarine deposition of wind blown volcanic ash from the Appalachian region. Kolata *et al.* (1983) investigated four such beds in Wisconsin, Iowa and Minnesota. They found that by means of chemical techniques (neutron activation and X-ray fluorescence) and statistical treatment (step-wise discriminant analysis) they could "fingerprint" each of the four K-bentonite beds at the 100% confidence level based on the most important trace elements including Co, Dy, Na, Sm, As and Cr. This investigation demonstrated the time-line character of K-bentonites and their fundamental use for correlation within the Galena Group.

METHODS OF STUDY

The study area is located along the Mississippi River in Iowa, Wisconsin, Illinois and Missouri (Figure 2). Six stratigraphic sections and four cores were chosen on the basis of availability, accessibility, and in order to adequately cover the wide geographic distribution, the lithologic variability and the change in thickness of the Galena Group. They have been described in detail by Bakush (1985). A total of 1773 thin sections were prepared from samples collected at an average vertical interval of 15 cm for limestones, and 30 to 60 cm for dolomites. Although the aggregated thickness of investigated rocks was 415 m, the microfacies study was limited to 187 m of limestones.

The thin sections were studied by the microfacies technique described in detail by Diaby and Carozzi (1984). This method consists of tabulating and measuring the indices of clasticity and frequency of all organic and inorganic detrital components and frequency of all benthic and planktic organic components (whole or fragmented) of carbonate rocks. In this study, the clasticity index was measured only for silt-size detrital quartz, pellets and intraclasts transported by weak currents. For the size of crinoid fragments (including echinoderms in general) which appear to represent an essentially *in situ* fauna together with other benthic constituents, the designation of "grain-size" rather than clasticity is used.

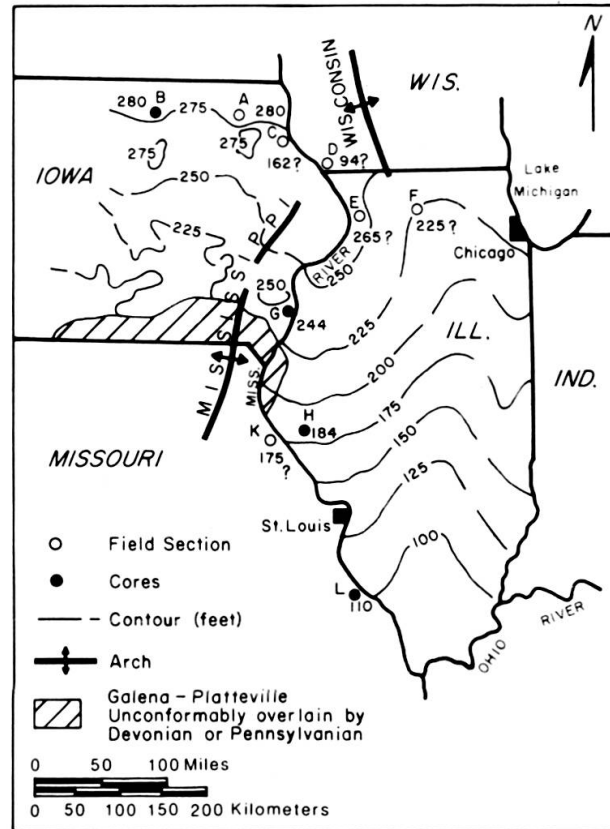


FIG. 2.

Isopach map of Galena Group (modified from Willman *et al.*, 1975 and Witzke, 1983) and location of sections.

The frequency index of the following components: detrital quartz, pellets, intraclasts, crinoids, bryozoans, brachiopods, gastropods, trilobites, ostracods, pelecypods, cephalopods and dasyclads, was determined over a standard surface area of 230.8 square mm consisting of six juxtaposed fields of view of the thin section at low magnification. The total of the six fields was considered the frequency of the component being counted. The relative abundance of minor components and of depositional textures that could not be statistically counted and measured but are important for environmental interpretation were recorded by visual estimation of their relative abundance in four classes: rare (< 1%), present (1-5%), common (5-10%) and abundant (> 10%).

The amounts of matrix, cement, dolomite and clay minerals were also estimated visually in percentage of all components in six fields of the thin section surface.

The statistical validity of the microfacies was evaluated with the Iterim subroutine of the iterative classification program of Demirmen (1969) by means of the IBM 360/75 computer at the University of Illinois. The SOUPAC (1976) statistical package allowed to calculate average values of all measured parameters in each microfacies

TABLE 1.
Average values of components per microfacies.

Components	1	2	3	4	5	6	7
Crinoid Freq.	26.3	14.1	86.0	137.0	105.0	168.3	188.3
Crinoid Size (mm)	0.5	0.7	1.0	1.12	1.12	1.36	1.5
Pellet Freq.	11.3	3.2	25.3	41.2	43.5	8.8	9.32
Pellet Clast. (mm)	0.017	0.02	0.032	0.04	0.077	0.04	0.035
Fine quartz Freq.	103.7	106.0	154.0	237.0	20.0	3.6	9.0
Fine quartz Clast. (mm)	0.037	0.04	0.045	0.15	0.04	0.02	0.05
Intraclast Freq.	0.09	0.44	3.3	3.08	6.79	3.5	6.31
Intraclast Clast. (mm)	0.02	0.03	0.07	0.12	0.23	0.16	0.2
Bryozoan Freq.	1.1	13.8	3.5	3.5	16.3	32.9	31.8
Brachiopod Freq.	17.3	128.7	40.1	34.3	47.4	16.3	37.6
Gastropod Freq.	3.0	8.7	11.0	15.8	15.2	0.47	2.7
Trilobite Freq.	4.6	15.1	6.9	9.9	11.1	2.8	12.4
Ostracod Freq.	8.4	10.0	9.4	9.0	12.6	1.5	11.2
Pelecypod Freq.	2.5	3.1	3.2	2.5	2.4	0.33	0.46
Dasyclad Freq.	0.26	0.0	3.9	10.5	0.94	0.0	0.43
Clay Minerals %	4.6	2.7	0.11	0.8	0.31	0.0	0.0
Calcsiltite Matrix %	77.6	55.3	64.2	41.4	29.7	10.4	5.1
Sparite Cement %	4.4	15.5	3.4	5.1	32.4	37.5	44.9
Bioturbation %	21.0	25.0	49.0	49.0	63.4	6.5	18.3

(Table 1). The table of average values of components was in turn used to calculate Pearson multivariate correlation coefficients between microfacies (Table 2). This table shows a very good correlation between microfacies 3 to 7, but displays low correlation between microfacies 1, 2 and 3; this is attributed to the unique character of the bioaccumulated limestone (microfacies 2) which does not correlate with the underlying microfacies 1 and overlying microfacies 3.

TABLE 2.

Multivariate correlation coefficients of microfacies.

Microfacies	1	2	3	4	5	6	7
1	1.000						
2	.475	1.000					
3	.773	.492	1.000				
4	.512	.262	.920	1.000			
5	.462	.390	.890	.937	1.000		
6	.225	.161	.692	.870	.831	1.000	
7	.274	.080	.680	.863	.792	.989	1.000

The combination of the correlation coefficients of microfacies and their vertical superposition in the field led to the recognition of a vertical shallowing-upward sequence which was then interpreted horizontally as a depositional model according to Walther's Law. The relative thickness of the microfacies in the shallowing-upward sequence and their relative horizontal extent in the depositional model are shown on their respective graphic representation and based on the average thickness in percent of each microfacies in the field columns.

DESCRIPTION OF MICROFACIES

The petrographic study led to the identification of seven microfacies which are described in order of increasing relative energy and general shallowing.

Microfacies 1 (Plate 1, A)

Moderately bioturbated and slightly pelletoidal calcisiltite with up to 10% scattered sand-size bioclasts of crinoids, brachiopods, ostracods, trilobites, gastropods, pelecypods, bryozoans, dasyclads, and *Receptaculites*. Calcified monaxonic and tetraxonic sponge spicules as well as fecal pellets are common. Bioturbation consists mostly of horizontal burrows often represented by concentrations of “flowery” pseudosparite or aggregates of dolomite rhombs.

Microfacies 2 (Plate 1, B)

Moderately bioturbated mud-supported to grain-supported brachiopod-pelecypod bioaccumulated limestone with calcisiltite matrix. Most of the shells are aligned parallel to bedding with common “umbrella” effects of sparite cement beneath them. However, local bioturbation has disrupted the original texture. Frequent whole gastropods are associated with bioclasts of bryozoans, crinoids, trilobites, and ostracods.

Microfacies 3 (Plate 1, C)

Moderately to heavily bioturbated mud-supported biocalcarenite with pelletoidal calcisiltite matrix. Bioclasts of crinoids and brachiopods predominate over gastropods, ostracods, trilobites, *Receptaculites*, dasyclads, bryozoans, and monaxonic sponge spicules. Bioturbation is expressed by abundant scattered patches of pseudosparite within the matrix.

Microfacies 4 (Plate 1, D)

Heavily bioturbated grain-supported biocalcarenite with pelletoidal calcisiltite matrix and rare sparite cement. Bioclasts of crinoids and brachiopods predominate over gastropods, *Vermiporella*, trilobites, ostracods, bryozoans, pelecypods, and *Receptaculites*. Calcisiltite intraclasts and fine grains of detrital quartz are conspicuous. Bioturbation consists of numerous burrows often filled by pseudosparite or aggregates of fine euhedral dolomite crystals.

Microfacies 5 (Plates 1, E and F, 2, 3)

Bioturbated and disorganized grain-supported biocalcirudite with sparite cement and rare pelletoidal calcisiltite matrix. Bioclasts of brachiopods, pelecypods, and crinoids dominate over common bryozoans, gastropods, ostracods, trilobites, dasyclads, and *Receptaculites*. The larger bioclasts are oriented in various directions, often imbricated and even perpendicular to bedding expressing the effects of violent reworking. Single valves of brachiopods and pelecypods occur in a horizontal or weakly inclined position with associated “umbrella” effects. In many instances, the finer bioclasts display an incipient graded bedding with interstitial material changing upward from sparite cement into pelletoidal calcisiltite matrix. The lower contact of the beds of microfacies 5 are often of erosional nature with scouring and clasts from the underlying lithology whereas the upper contacts are always gradational. The combination of these features indicates a storm origin. Bioturbation may introduce locally further disruption of the depositional textures.

Microfacies 6 (Plates 1, G, 5, 6)

Moderately bioturbated coarse grain-supported to pressure-welded crinoid-bryozoan calcarenite with sparite cement and rare calcisiltite matrix. Associated with the predominant bioclasts are brachiopods, trilobites, ostracods, gastropods, pelecypods, and *Receptaculites*. This microfacies is finer grained than the preceding one and less disorganized although entire valves and bioclasts display variable orientations, imbrication, and frequent incipient graded-bedding. All other sedimentary textures are similar to those of microfacies 5 and indicate a storm origin of lesser intensity also modified by subsequent bioturbation.

Microfacies 7 (Plate 1, H)

Moderately bioturbated grain-supported to pressure-welded crinoid-brachiopod-bryozoan calcarenite with hematitic sparite cement. Crinoid columnals are well-sorted and strongly abraded while bryozoans are highly fragmented. They are associated with bioclasts of trilobites, ostracods, gastropods, pelecypods, dasyclads, *Receptaculites*, corals, and an appreciable amount of calcisiltite intraclasts. Cementation combines syntaxial overgrowths on crinoid columnals and interparticle equant sparite mosaic.

IDEAL FAIR-WEATHER-STORM SHALLOWING-UPWARD SEQUENCE

The analysis of the stratigraphic columns and the correlation coefficients between the various microfacies indicate that microfacies 1, 2, 3, 4, and 7 are fair-weather deposits which build an ideal shallowing-upward sequence (Figure 3) with the statistically most frequent intercalation of microfacies 5 (high energy tempestite) between 3 and 4 and the intercalation of microfacies 6 (medium energy tempestite) between 4 and 7. The variation of the microscopic parameters are shown as continuous curves for the ideal shallowing-upward sequence of fairweather microfacies whereas the corresponding values for the intercalated storm microfacies are indicated by individual peaks (Figure 3). This mode of representation allows to compare the effects of storm processes on the fair-weather sedimentation. The detailed variations of the microscopic parameters are shown in two instances of superposed shallowing-upward sequences (Figures 4, 5, 6) taken from the detailed description of all the investigated sections (Bakush, 1985).

IDEAL FAIR-WEATHER-STORM DEPOSITIONAL MODEL

The proposed depositional model (Figures 7, 8) represents a shallow infratidal and open marine carbonate ramp submitted to episodic storm action. Morphologically it may be divided from N to S into three environments: a slope, an extensive outer platform with incipient bioaccumulation at the distal end, and a shoal.

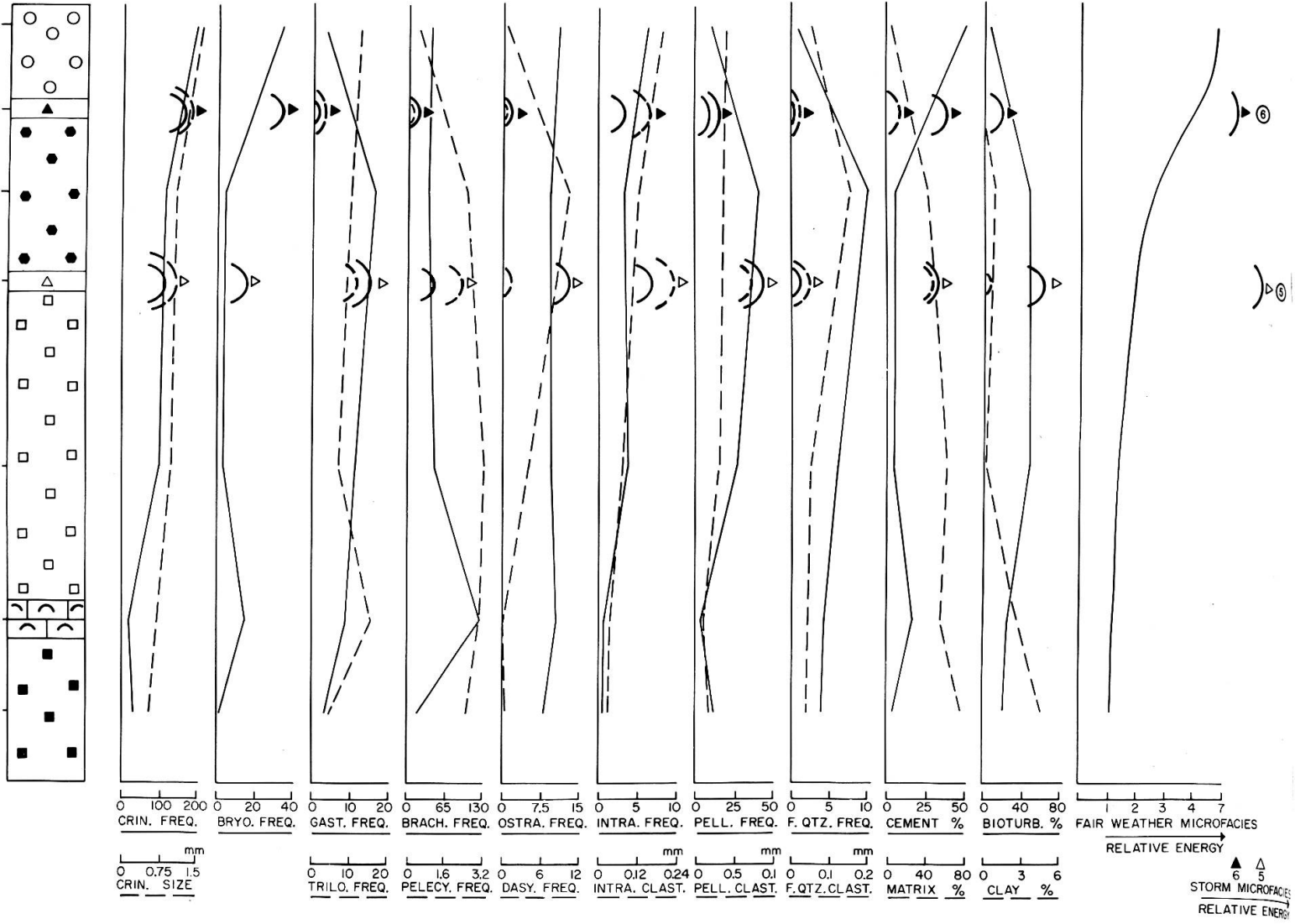


FIG. 3.

Ideal shallowing-upward sequence.

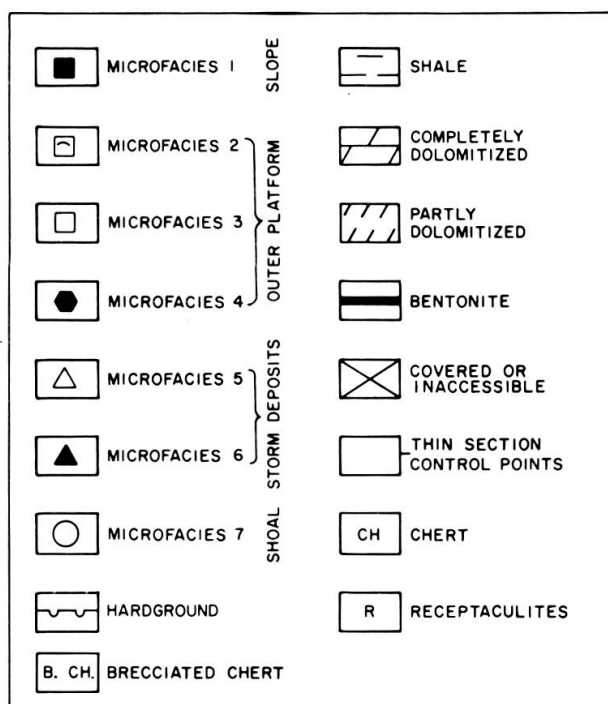


FIG. 4.

Symbols for microfacies and diagenesis.

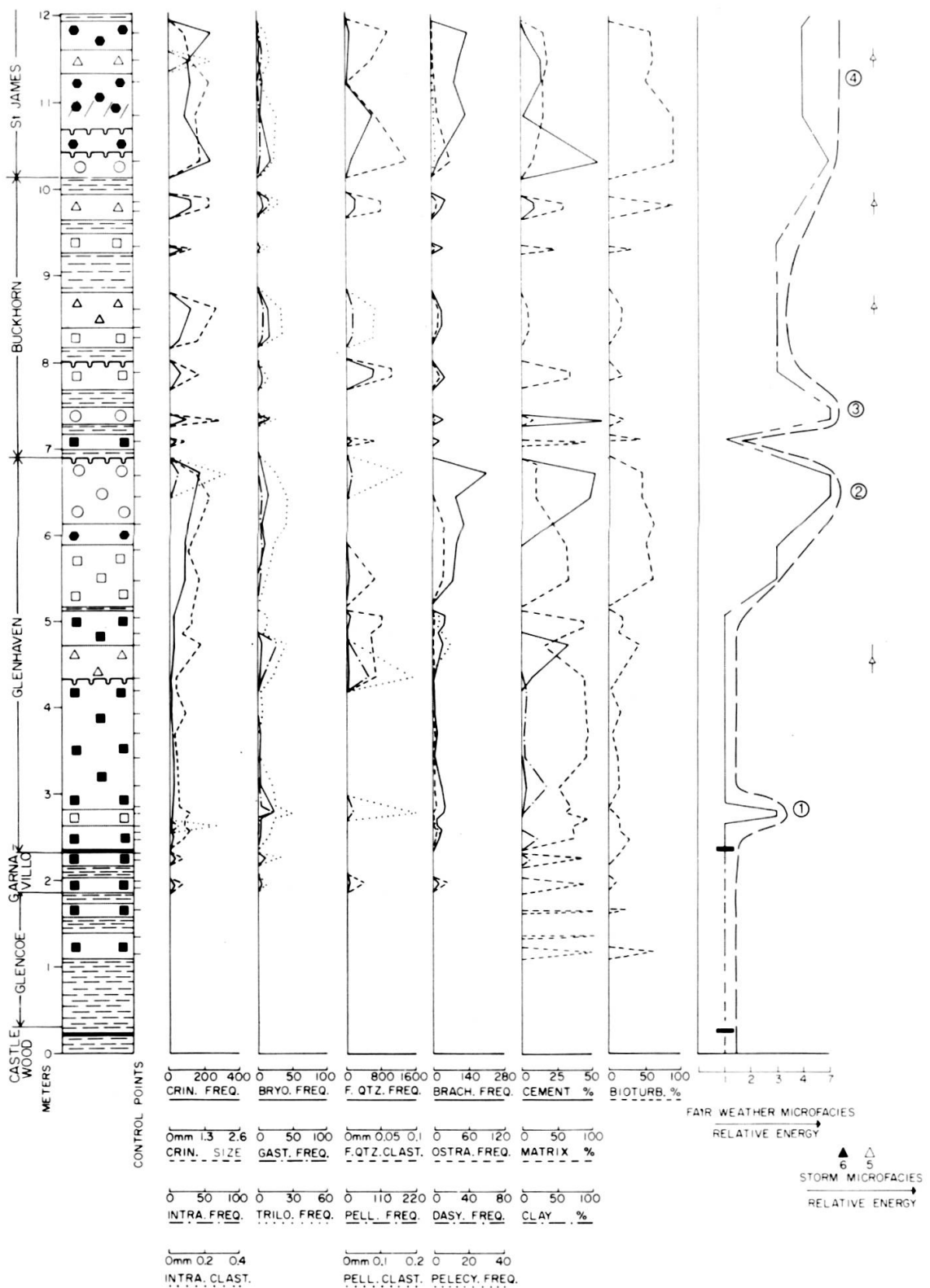


FIG. 5.

Typical example of variations of microscopic parameters in a shallowing-upward sequence, field section C near Guttenberg, Iowa (0 to 12 m).

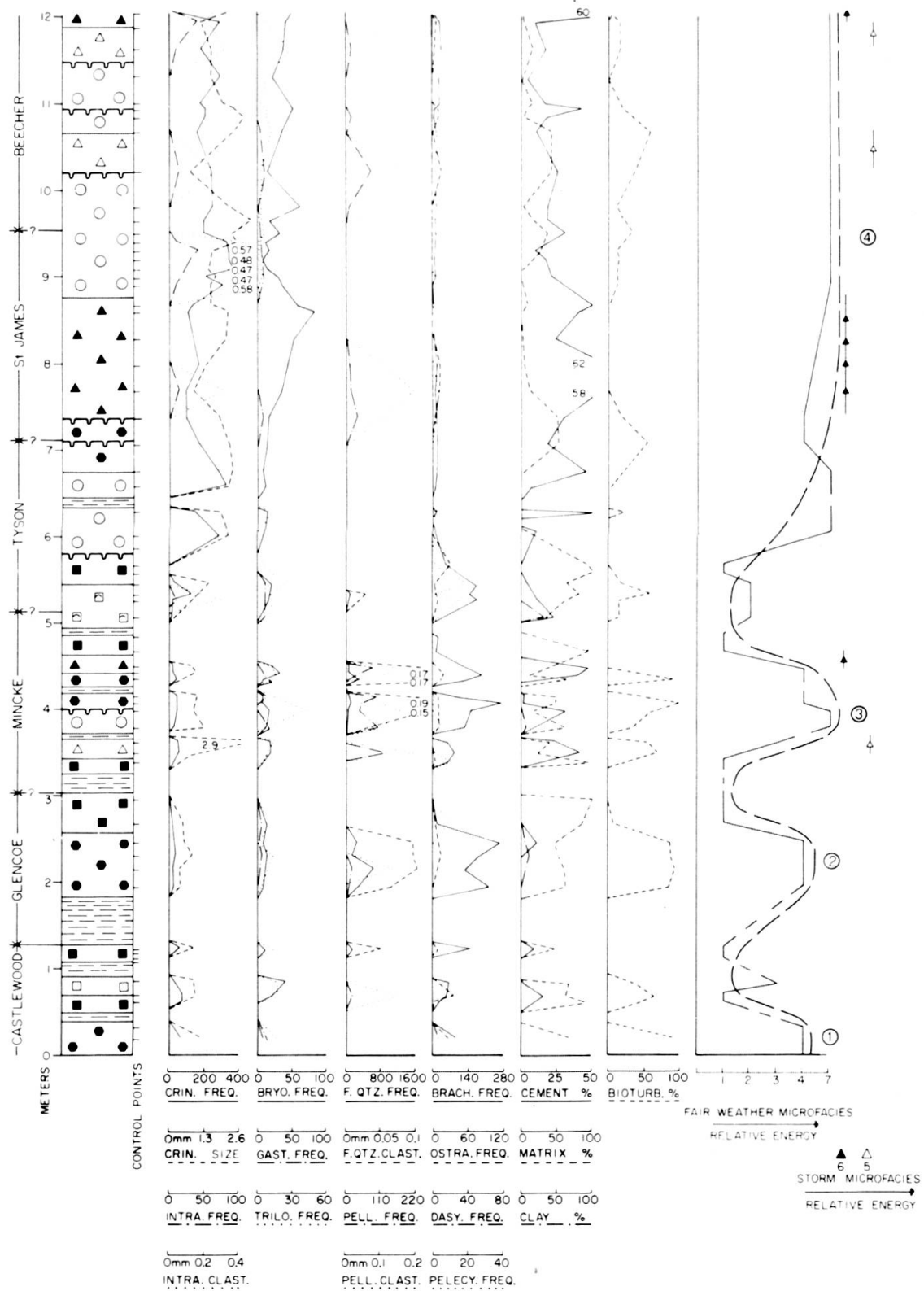


FIG. 6.

Typical example of variations of microscopic parameters in a shallowing-upward sequence, core section L near Bloomsdale, Missouri (0 to 12m).

The expected more shoreward environments were not detected in the studied area because of the great extent of the Galena sea over the American Midcontinent which led to the shorelines being far to the west-southwest and the north.

The behavior of most of the benthic constituents of the fair-weather microfacies such as crinoids, bryozoans, gastropods, brachiopods, pelecypods, and *Receptaculites* shows *in situ* assemblages. This situation indicates that the carbonate ramp had a very gentle slope and paleoecological data mainly based on the living conditions of *Receptaculites* lead to estimate the maximum water depth of the proposed model at about 60 feet (18.3 m).

The frequency and size (not clasticity) of the debris released in place after death of the crinoids are at a peak in microfacies 7 and decrease gradually toward deeper and more quiet microfacies. The behavior of the two curves indicates that abundant and large species of crinoids were living in the shallow and high energy shoal environment and that with increasing depth, crinoids became smaller, more delicate, and less abundant. Other evidences of the autochthonous character of the fauna are as follows: two distinct assemblages of bryozoans in the shoal area (microfacies 7) and in the distal part of the outer platform (microfacies 2) in coincidence with the bioaccumulation of the brachiopods; peak of gastropods in the proximal part of the outer platform (microfacies 4); and finally maximum frequency of the pelecypods in microfacies 3 with a curve following a trend entirely different from that of the other constituents.

The weak currents flowing downslope and decreasing in intensity in that direction are responsible for the local intraformational generation of intraclasts and lithic pellets from freshly deposited, semi-indurated muds. This situation is expressed by the gradual and parallel decrease downslope of the clasticity and frequency of the intraclasts. The trend is slightly different for the pellets where a frequency peak in microfacies 4, in coincidence with the frequency peak of the gastropods and of the intensity of bioturbation, may indicate an addition of fecal pellets.

The same weak currents distribute silt-size grains of detrital quartz with a gradual decrease of clasticity and frequency downslope preceded by lows in microfacies 7 indicating that these small particles could not remain in high energy conditions and were winnowed away. In a similar manner, the clay minerals increase in amount downslope and eventually settle in the deepest environment.

Storm deposits of microfacies 5 and 6 consist of materials originating from nearby fair-weather microfacies. This local derivation can be shown by the estimation in percentage of the number of times that storm microfacies 5 and 6 rest, in the field sections and cores, on the fair-weather microfacies (1, 2, 3, 4, and 7). Microfacies 5 rests 15%, 15.2%, 20.3%, 46%, and 3.5% on fair-weather microfacies 1, 2, 3, 4, and 7, respectively, while microfacies 6 rests 36% and 64% on fair-weather microfacies 4 and 7, respectively. Therefore, in the ideal depositional model, the location of the storm microfacies is based on the highest percentage. Thus, microfacies 5 is located between 3 and 4, corresponding to the highest intensity storm action accompanied by the

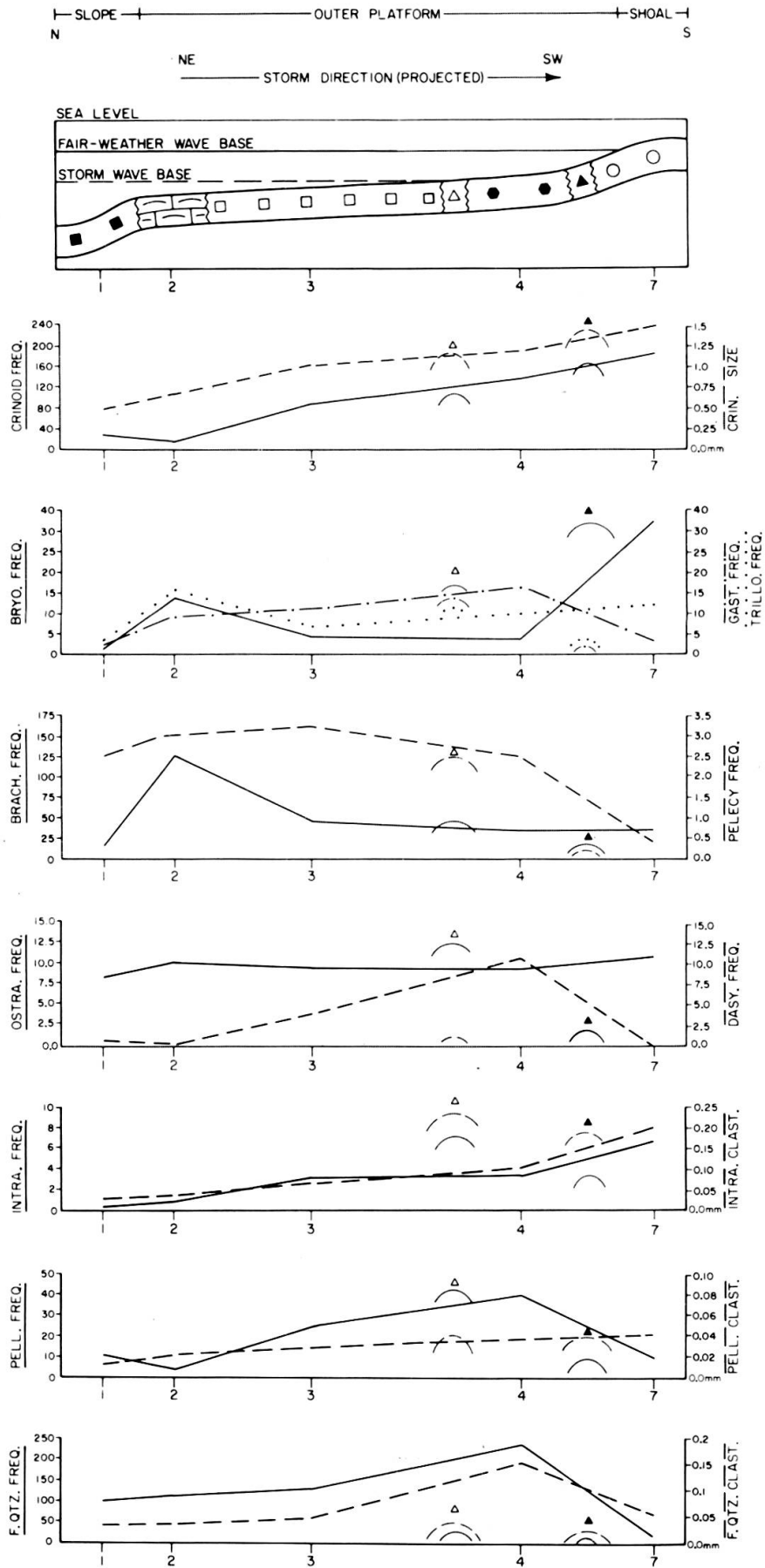


FIG. 7.
Fair-weather-storm depositional model.

maximum lowering of storm wave base, whereas microfacies 6 is located between 4 and 7, corresponding to lower intensity storm action. Both types of tempestites display textures indicating processes which put the constituents of the fair-weather microfacies into suspension and redeposited them essentially in place, or within a short distance. Apparently, storm-induced turbidites due to backflow currents were not generated, perhaps due to the very gentle slope of the carbonate ramp. If they had been generated, the above relations of percentages would not occur.

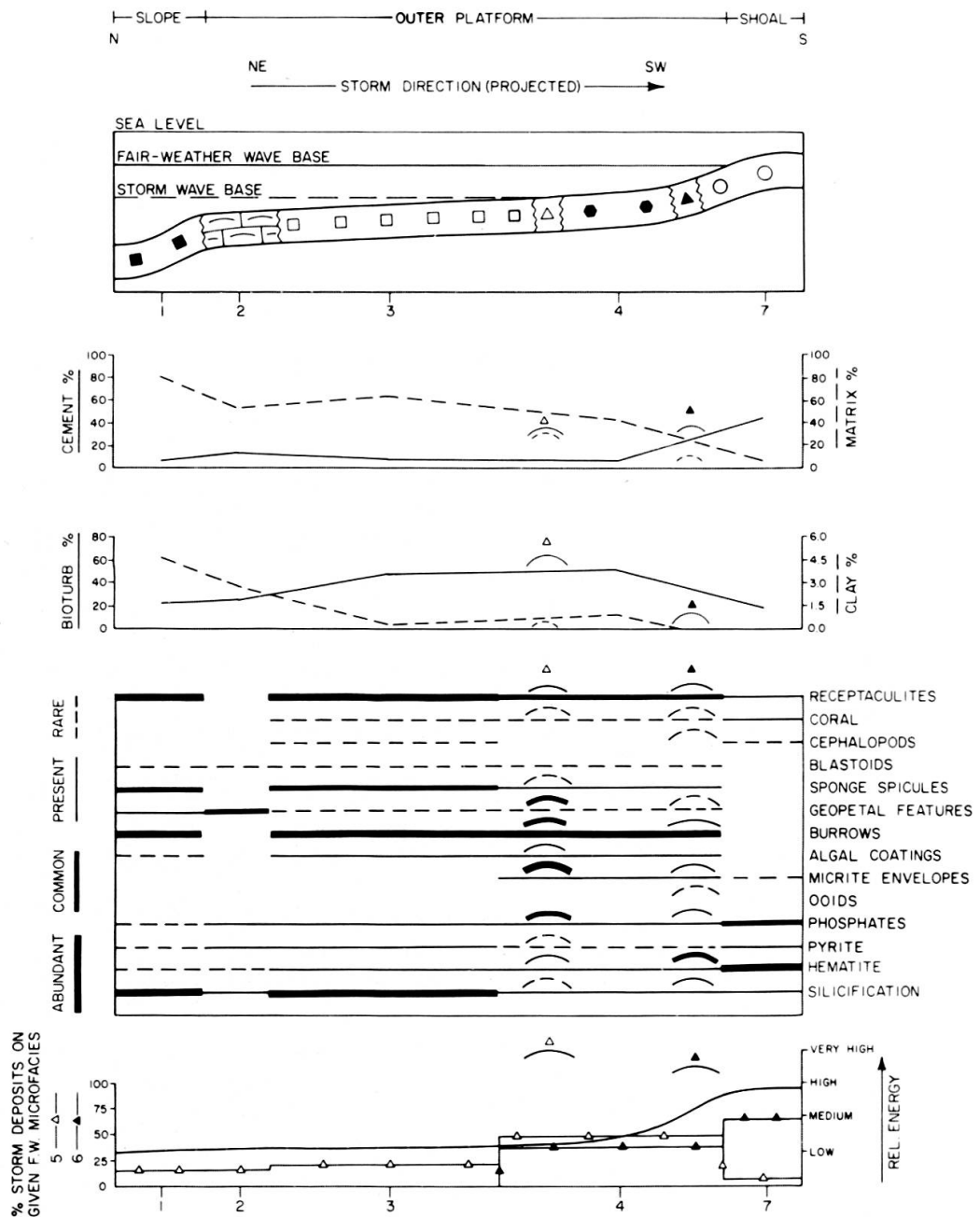


FIG. 8.

Fair-weather-storm depositional model (continued).

A comparison of the behavior of the various parameters between fair-weather conditions and storm conditions indicates that in the case of the highest intensity tempestite (microfacies 5), most of the constituents increase in frequency by mechanical concentration except the sturdy or heavy organisms (gastropods and pelecypods) which were apparently not appreciably affected by the process. In the tempestite of lesser intensity (microfacies 6), most of the constituents decrease significantly in frequency or remain unchanged indicating winnowing or a simple reorganization.

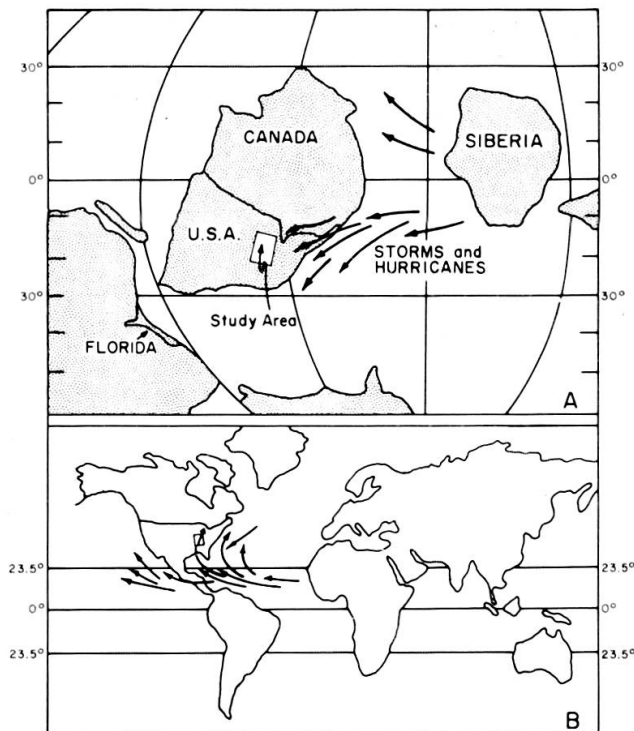


FIG. 9.

Comparison of possible storm tracks of hurricanes during Middle Ordovician (A) and at present (B). Modified from Kreisa (1981).

The storms were reaching first the deeper areas of the Galena sea in the north and then the shallower areas to the south (Figures 7, 8). The most violent effect on the sediment-water interface occurred, therefore, in the proximal part of the outer platform where the storm wave base first intersected the sea floor, generating the disorganized calcirudite of microfacies 5. As the storms moved to the southern part, transition outer platform-shoal, they decreased in intensity and generated the graded bedded calcarenites of microfacies 6.

Examination of the field sections and cores shows that storm deposits increase in number from north to south toward the shallower environment. The sea floor in the deeper northern area is inferred to have been only affected by the stronger storms, whereas the shallower southern area would also have been affected by weaker storms, thus displaying a greater recorded number of storm deposits than in the north.

The literature indicates that during Middle and Upper Ordovician, major storms surged over the North American continent (Kreisa, 1981). Paleogeographic reconstructions by Scotese *et al.* (1979) and Ziegler *et al.* (1979) show that during the Ordovician the study area was located approximately between 10-20° latitude south and was rotated about 30 to 45° compared to its present orientation (Figure 9A). The path of present day storms appears to be the mirror image of those in Ordovician time (Figure 9B). The storms of the Middle and Upper Ordovician may well have originated in the oceanic basin east of North America, moved to the west, and then were deflected mainly to the southeast and northwest around the high pressure system of the American continent.

GENERAL EVOLUTION OF THE DEPOSITIONAL ENVIRONMENTS

A composite section of the investigated limestone portion of the Galena Group (Figure 10) shows that it consists of twenty-five environmental oscillations displaying a broad range of amplitude and an association of asymmetric (shallowing-upward) and symmetric types (shallowing- and deepening-upward). It is generally observed that in carbonates, the shallower environments tend to record a greater number of oscillations than the deeper ones during a given time interval. In the Galena, just the opposite occurs (Figure 11). This is probably due to the fact that the relatively deep infratidal environment in the north consists of different microfacies whereas the relatively shallower infratidal environment in the south consists only of crinoidal-bryozoan microfacies.

Since the Galena Group corresponds to a fair-weather-storm depositional model, a cross section from north to south can be drawn to show the relationships between the environmental oscillations and the pattern of distribution of storms (Figure 11). At least five successive alternating predominant storm- and fair-weather episodes can be outlined. The boundaries of these episodes were established by the presence or absence of single and/or combined storm events in the different sections and independently from any lithostratigraphic correlations. An examination of episodes I, II, and V which are storm-dominated illustrates clearly that the type of predominant tempestite changes from N to S, from microfacies 5 to 6, and that simultaneously the overall number of recorded events increases. Detailed correlations have shown tempestites (microfacies 5), 10 to 12 cm thick, continuously traceable for more than 48 miles (77 km).

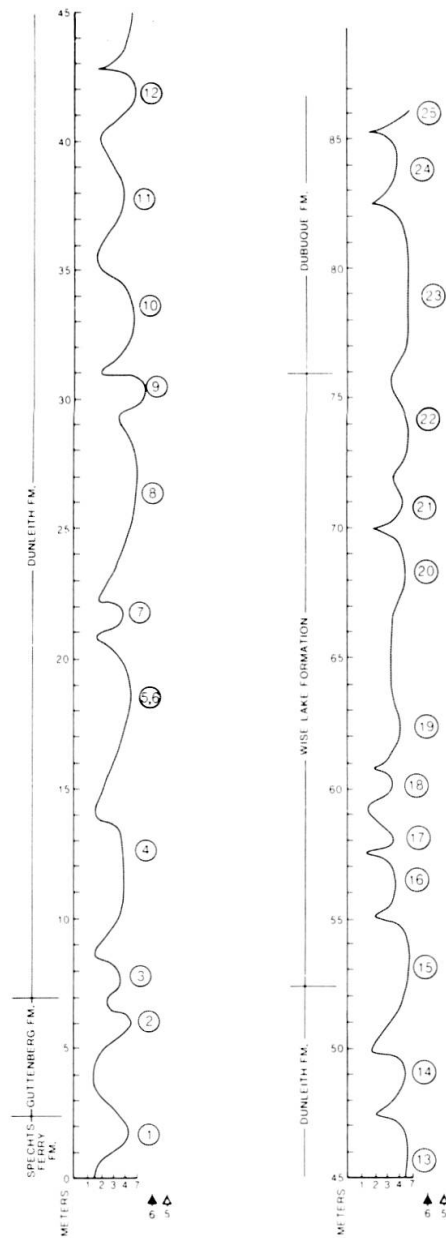


FIG. 10.

Composite section of the cycles of Galena Group (0 to 7 m, section D; 7 to 52.40 m, section A, and 52.40 to 86.15 m, section B).

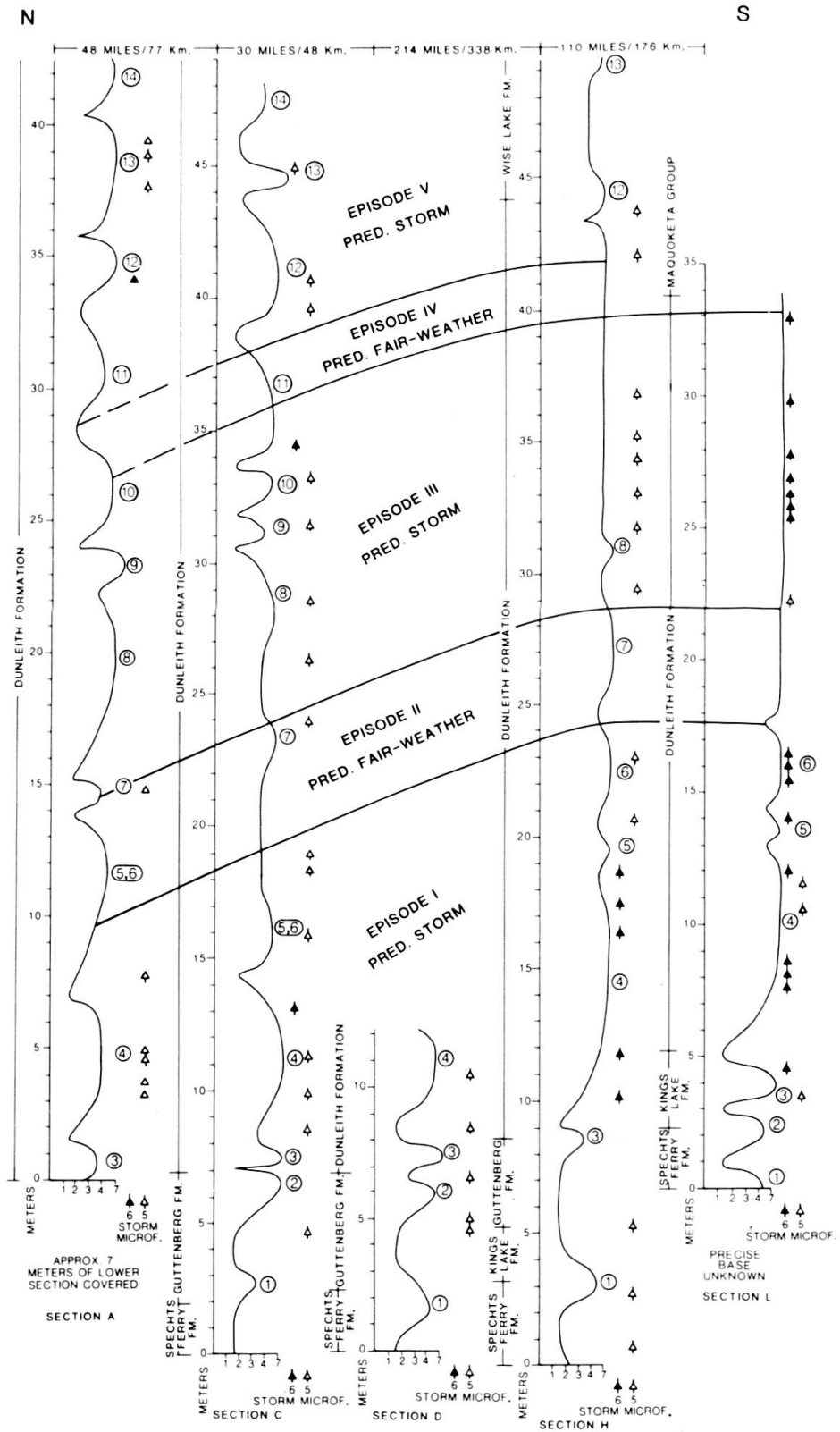


FIG. 11.

North-south tentative environmental correlation by cycles, and by fair-weather-storm episodes of Galena Group. Note that cycles decrease in number from north to south.

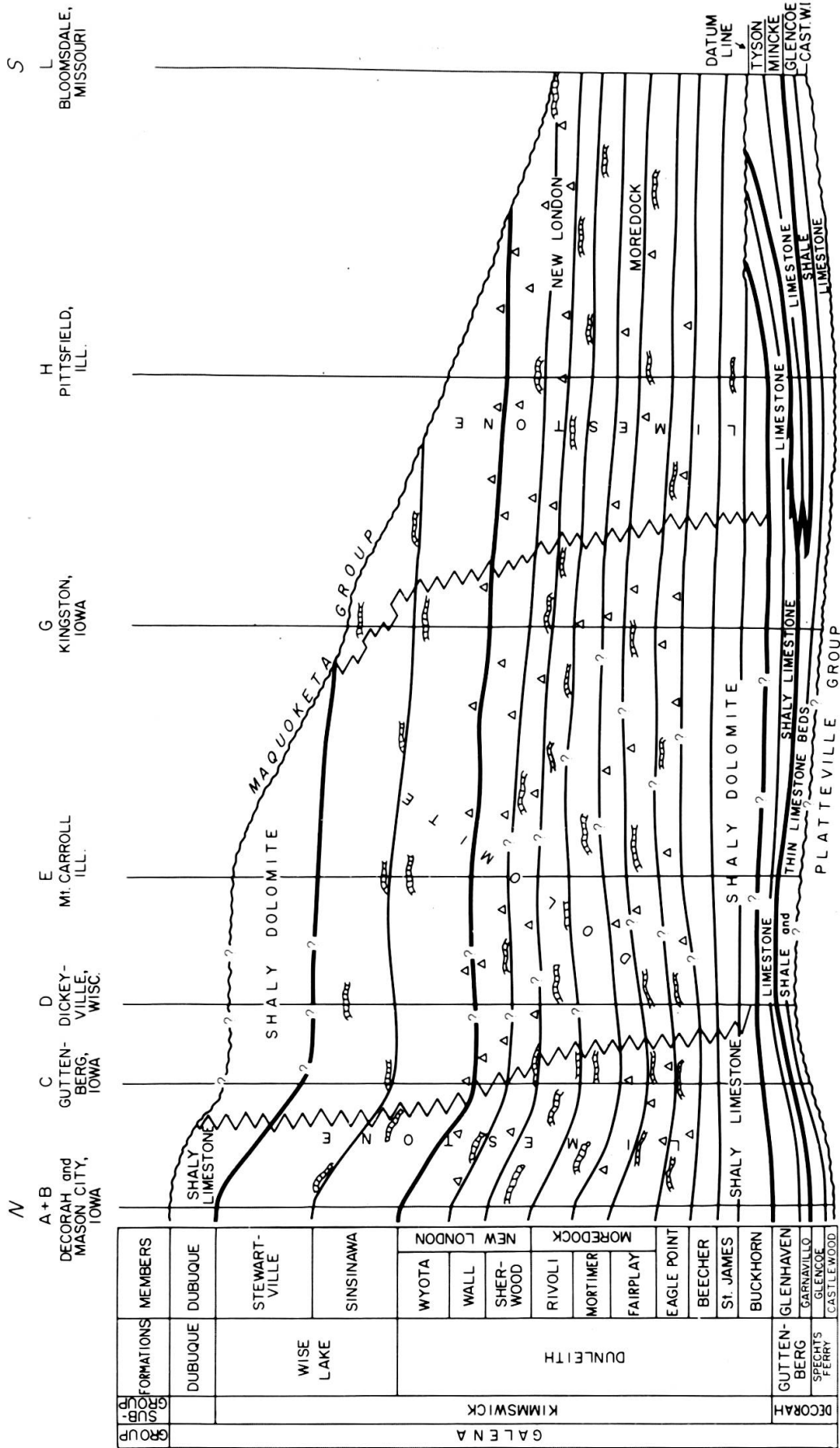


FIG. 12.

North-south lithostratigraphic cross section of Galena Group in study area (see Figure 1 for symbols).

DIAGENETIC EVOLUTION

The Galena Group has been extensively dolomitized in northern Illinois and eastern Iowa by a large-scale Dorag mechanism leading to a concentration of dolomite in the central part of the study area surrounded by limestone (Figure 12). Therefore, the description of the diagenetic evolution concerns first the limestones and then the dolomites.

Diagenetic Evolution of the Limestones

The observed features and their time relationships (Figure 13, Plate 6) reveal a fairly complex evolution with some phases deserving additional comments. Extensively bioturbated calcisiltites display burrows with concentrations of fine to medium euhedral rhombs of dolomite (Plate 6, A). This early submarine dolomitization was apparently controlled by permeability inhomogeneities within the burrows and the needed magnesium may have been provided by organic constituents such as minute crinoid bioclasts, and subsequently concentrated in solutions.

An unusual combination of early submarine silicification and of storm effects is revealed by ellipsoidal chert nodules rotated and imbedded in crinoidal calcisiltites which themselves display a soft pebble monogenic brecciated texture (outcrop on Highway 9, Decorah, Iowa) described in detail by Bakush (1985). Some of the chert nodules are either partly or completely broken in place with the country rock filling the space between the fragments, while others appear shattered into numerous minute polyhedral fragments (Plate 7). These unusual chert nodules demonstrate the following succession of events: 1. Deposition of crinoidal calcisiltite bed; 2. Syngenetic submarine silicification generating completely indurated but easily fracturable chert nodules by replacement of the host sediment; 3. High energy storm event which uplifted, rotated, and transported the chert nodules for a short distance, breaking them in various ways, while simultaneously reworking the semi-consolidated host sediment into a soft pebble monogenic breccia; 4. Final deposition by gravity of all the constituents.

A very similar case of syngenic chert breccia in the Burlington Limestone was interpreted as a Mississippian tempestite (Carozzi and Gerber, 1978).

Hardgrounds (Plate 6, B, C) are extremely common in the investigated rocks. They are smooth to highly irregular surfaces of discontinuity between two microfacies or inside the same microfacies due to chemical dissolution of early submarine cemented sediment accompanied by various types of mineralization (hematite, pyrite, phosphates), or non-deposition, or submarine mechanical erosion.

A second phase of silicification expressing a mixed marine freshwater phreatic environment is represented by a megaquartz mosaic filling cavities formed by dissolution of an equant calcite mosaic of previous freshwater phreatic origin.

DIAGENETIC ENVIRONMENTS DIAGENETIC FEATURES	MARINE PHREATIC	UNDERSATURATED FRESHWATER PHREATIC	SATURATED FRESHWATER PHREATIC	MIXING MARINE FRESHWATER PHREATIC	BURIAL
BIOTURBATION (BURROWS AND BORING OF BIOCLASTS)	————				
EARLY SUBMARINE DOLOMITIZATION	————				
SILICIFICATION (I) (EARLY SUBMARINE)	————				
HARDGROUNDS WITH IRON IMPREGNATION	————				
SYNERESIS	————				
MICRITIZATION (ALGAL COATINGS AND MICRITE ENVELOPES)	————				
INTERNAL SEDIMENTS (WITH GEOPETAL FEATURES)	————				
ISOPACHOUS RIM CEMENT	————				
EARLY COMPACTION	————				
LEACHING OF ARAGONITIC SKELETAL DEBRIS		————			
CAVITY FILLING SPARITE CEMENT			————		
SYNTAXIAL OVERGROWTH			————		
AGGRADING NEOMORPHISM (STABILIZATION OF RIM CEMENT)			————		
SILICIFICATION II				————	
LATE COMPACTION (STYLOLITIZATION)					————
MINERALIZATION (POST EARLY PERMIAN-PRE LATE CRETACEOUS)					————
LATE FRACTURATION					————
LATE FRACTURE FILLING CALCITE CEMENT					————
TIME					

FIG. 13.

Diagenetic features and environments of limestones of Galena Group.

Diagenetic Evolution of the Dolomites

The observed features and their time relationships (Figure 14, Plate 8) indicate that the limestones became extensively dolomitized after the second phase of silicification in the mixed marine freshwater phreatic environment. The isopachs of the dolomites formed by this regional Dorag model follow a SW-NE trend (Figure 15). The contours of the thickest dolomite occurrence correspond to the emergent part of the Galena Group between the Wisconsin Arch and the Mississippi River Arch which was exposed during or at the end of Maquoketa time (Late Ordovician), an episode of worldwide lowering of sea level (Vail *et al.*, 1977). A large active freshwater lens would have existed in this emergent area, leading in turn to the development of an extensive mixed marine-freshwater system. This interpretation which corresponds to the original Dorag model proposed by Badiozamani (1973) is favored by Delgado (1983), by Gregg and Sibley (1983), and with some reservations by Witzke (1983).

Petrographically, dolomitization displays three habits: fine anhedral crystals (0.01 to 0.12 mm) in calcisiltites; interlocking subhedral rhombs (0.03 to 0.24 mm) replacing calcisiltites and mud-supported biocalcarenites; zoned euhedral medium to coarse rhombs (0.22 to 0.24 mm) replacing grain-supported biocalcarenites. The occurrence of these habits reflects the grain size of the original carbonates.

A third phase of silicification follows dolomitization and consists of fibroradiated microcrystalline quartz replacing entirely or marginally dolomite rhombs, or euhedral quartz crystals replacing rhombs.

Uplifting of the major positive structures of the investigated area was reactivated during Champlainian times and may have continued later. Consequently, the dolomitized Galena Group was elevated and underwent a second diagenetic evolution before final burial (Figure 14). It consists of dedolomitization and of an interesting phase of pyrite mineralization which took place after late compaction, dissolving and replacing both coarse equant sparite cement and dolomite rhombs. The latter display severe marginal dissolution and show a "floating" texture within pyrite. This mineralization is an aspect of the Mississippi-type ore deposits for which an Illinois Basin brine hypothesis is favored at present (Bethke, 1986). The age of the mineralization is debated and considered to range from post Early Permian to pre Late Cretaceous; at any rate, the late vertical fracturation observed in the diagenetic sequence of the dolomites cuts pyrite seams.

CONCLUSIONS

The carbonate rocks of the Galena Group consist of five distinct fair-weather microfacies which represent a shallow open marine subtidal carbonate ramp composed of the following environments: slope (microfacies 1); outer platform (microfacies 2, 3 and 4); and shoal (microfacies 7). The model displays its deepest part

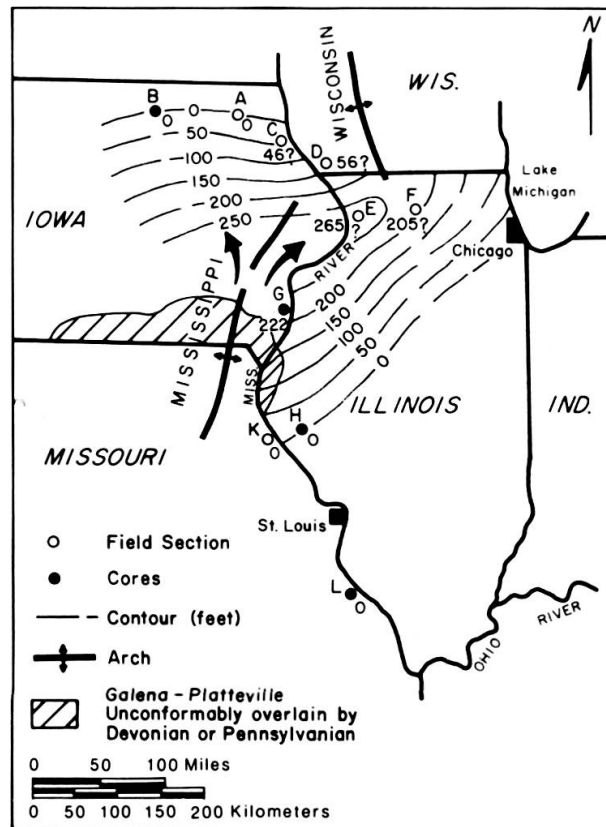


FIG. 15.

Isopach map of dolomite of Galena Group. Arrows around Mississippi River Arch are the possible pathways of circulation of mixed marine freshwater of the Dorag model of dolomitization.

and its shallowest one in the northern and southern parts of the study area, respectively. It is an incomplete model because the more shoreward fair-weather environments (inner platform, intertidal, shoreline, and supratidal) are not present since the Galena sea covered most of the North American continent and the shoreline was far from the study area.

Storm action interfered with the fair-weather microfacies of the shallower portion of the outer platform and with the shoal. When storm wave base hit the sea floor, a disorganized biocalcirudite with sparite cement (microfacies 5) was generated, but as the storms decreased in intensity southward, a less disorganized and graded bedded biocalcarenite with sparite cement (microfacies 6) was deposited.

The generalized environmental evolution shows that the Galena Group consists of twenty-five symmetrical and asymmetrical cycles. The oscillations are more numerous in the deeper part to the north because more microfacies exist in such low and medium energy environments than occur in the higher energy environments of the shallower southern part. Based on the depositional cycles and the pattern of storms, at least five successive predominant storm and fair-weather episodes are distinguished. The recorded storms generally increase in number from north to south toward the shallow

environment. The sea floor in the deeper northern area is inferred to have been affected only by the stronger storms, whereas the shallower southern area would also have been affected by weaker storms, thus displaying a greater recorded number of storm deposits than in the northern area.

The petrographic investigation revealed the presence of the following diagenetic environments: 1) marine phreatic (bioturbation, early submarine dolomitization, silicification I with breccia, hardgrounds, syneresis cracks, micritization, internal sediments, isopachous rim cement and early compaction); 2) undersaturated freshwater phreatic I (leaching of aragonitic skeletal debris); 3) saturated freshwater phreatic I (cavity filling sparite cement, syntaxial overgrowth cement and neomorphism); 4) mixed marine-freshwater phreatic (silicification II, large scale dolomitization of Dorag type and silicification III); 5) tectonic uplift stage which caused the dolomites to undergo another diagenetic sequence; 6) undersaturated freshwater phreatic II (dedolomitization); 7) saturated freshwater phreatic II (poikilotopic calcite cement); and 8) burial (late compaction, stylolitization, mineralization of Mississippi Valley type and late burial fracturation and fracture filling calcite cement).

REFERENCES

- BADIOZAMANI, K. (1973). The Dorag dolomitization model—Application to the Middle Ordovician of Wisconsin: *Jour. Sed. Petrology*, 43, 4, 965-984.
- BAKUSH, S. H. (1985). Carbonate microfacies, depositional environments and diagenesis of the Galena Group (Middle Ordovician) along the Mississippi River (Iowa, Wisconsin, Illinois and Missouri), U.S.A.: *Unpubl. Ph. D. thesis, Univ. of Illinois (Urbana-Champaign)*, 223 p.
- BETHKE, C. M. (1986). Hydrologic constraints on genesis of the Upper Mississippi Valley Mineral District from Illinois Basin brines: *Economic Geology*, 81, 2, in press.
- CAROZZI, A. V. and M. S. GERBER (1978). Synsedimentary chert breccia: A Mississippian tempestite: *Jour. Sed. Petrology*, 48, 3, 705-708.
- DELGADO, D. J. (1980). Submarine diagenesis (aragonite dissolution, cementation by calcite, and dolomitization) in Ordovician Galena Group, Upper Mississippi Valley: *Amer. Assoc. Petrol. Geologists Bull. Abstracts*, 64, 5, 697.
- (1983). Deposition and diagenesis of the Galena Group in the Upper Mississippi Valley: in DELGADO, D. J. (ed.), Ordovician Galena Group of the Upper Mississippi Valley: Deposition, Diagenesis and Paleoecology: *Guidebook for the 13th Annual Field Conference, Great Lakes Section SEPM*, September 30-October 2, 1983, A1-A17.
- DEMIRMEN, F. (1969). Multivariate procedures and Fortran IV program for evaluation and improvement of classification: *Kansas State Geol. Survey Computer Contrib.*, 31, 51 p.
- DIABY, I., and A. V. CAROZZI (1984). The St. Louis Limestone (Middle Mississippian) of Illinois Basin, U.S.A.—A carbonate ramp-bar-platform model: *Archives des Sciences, Genève*, 37, 2, 123-169.
- GREGG, J. M., and D. F. SIBLEY (1983). Xenotopic dolomite texture—Implications for dolomite neomorphism and late diagenetic dolomitization in the Galena Group (Ordovician), Wisconsin and Iowa: in DELGADO, D. J. (ed.), Ordovician Galena Group of the Upper Mississippi Valley: Deposition, Diagenesis and Paleoecology: *Guidebook for the 13th Annual Field Conference, Great Lakes Section SEPM*, September 30-October 2, 1983, G1-G15.
- KOLATA, D. R., W. D. HUFF, and J. K. FROST (1983). Correlation of K-Bentonites in the Decorah Subgroup of the Mississippi Valley by chemical fingerprints: in DELGADO, D. J. (ed.), Ordovician Galena Group of the Upper Mississippi Valley: Deposition, Diagenesis and Paleoecology: *Guidebook for the 13th Annual Field Conference, Great Lakes Section SEPM*, September 30-October 2, 1983, F1-F15.

- KREISA, R. D. (1981). Storm-generated sedimentary structures in subtidal marine facies with examples from the Middle and Upper Ordovician of southwestern Virginia: *Jour. Sed. Petrology*, 51, 3, 823-848.
- SCOTESE, C. R., R. K. BAMBACH, C. BARTON, R. VAN DER VOO, and A. M. ZIEGLER (1979). Paleozoic base maps: *Jour. Geology*, 87, 3, 217-277.
- SOUPAC (1976). Soupac program descriptions, vol. 1, C.S.O., *University of Illinois*, Urbana-Champaign.
- TEMPLETON, J. S., and H. B. WILLMAN, 1963. Champlainian Series (Middle Ordovician) in Illinois: *Illinois State Geol. Survey Bull.*, 89, 269 p.
- VAIL, P. R., R. M. MITCHUM, JR., and S. THOMPSON, III (1977). Seismic stratigraphy and global changes of sea level, part 4: Global cycles of relative changes of sea level: in PAYTON, C. E. (ed.), *Seismic stratigraphy—Applications to hydrocarbon exploration: Amer. Assoc. Petrol. Geologists Memoir* 26, 83-97.
- WILLMAN, H. B., E. ATHERTON, T. C. BUSCHBACH, C. COLLINSON, J. C. FRYE, M. E. HOPKINS, J. A. LINEBACK, and J. A. SIMON (1975). Handbook of Illinois stratigraphy: *Illinois State Geol. Survey Bull.*, 95, 261 p.
- WILLMAN, H. B., and D. R. KOLATA, 1978. The Platteville and Galena Group in Northern Illinois: *Illinois State Geol. Survey Circular*, 502, 75 p.
- WITZKE, B. J. (1983). Ordovician Galena Group in Iowa subsurface: in DELGADO, D. J. (ed.), *Ordovician Galena Group of the Upper Mississippi Valley: Deposition, Diagenesis, and Paleoecology: Guidebook for the 13th Annual Field Conference, Great Lakes Section SEPM*, September 30-October 2, 1983, D1-D26.
- ZIEGLER, A. M., C. R. SCOTESE, W. S. MCKERROW, M. E. JOHNSON, and R. K. BAMBACH (1979). Paleozoic paleogeography: *Ann. Rev. Earth Planet. Sci.*, 7, 473-502.

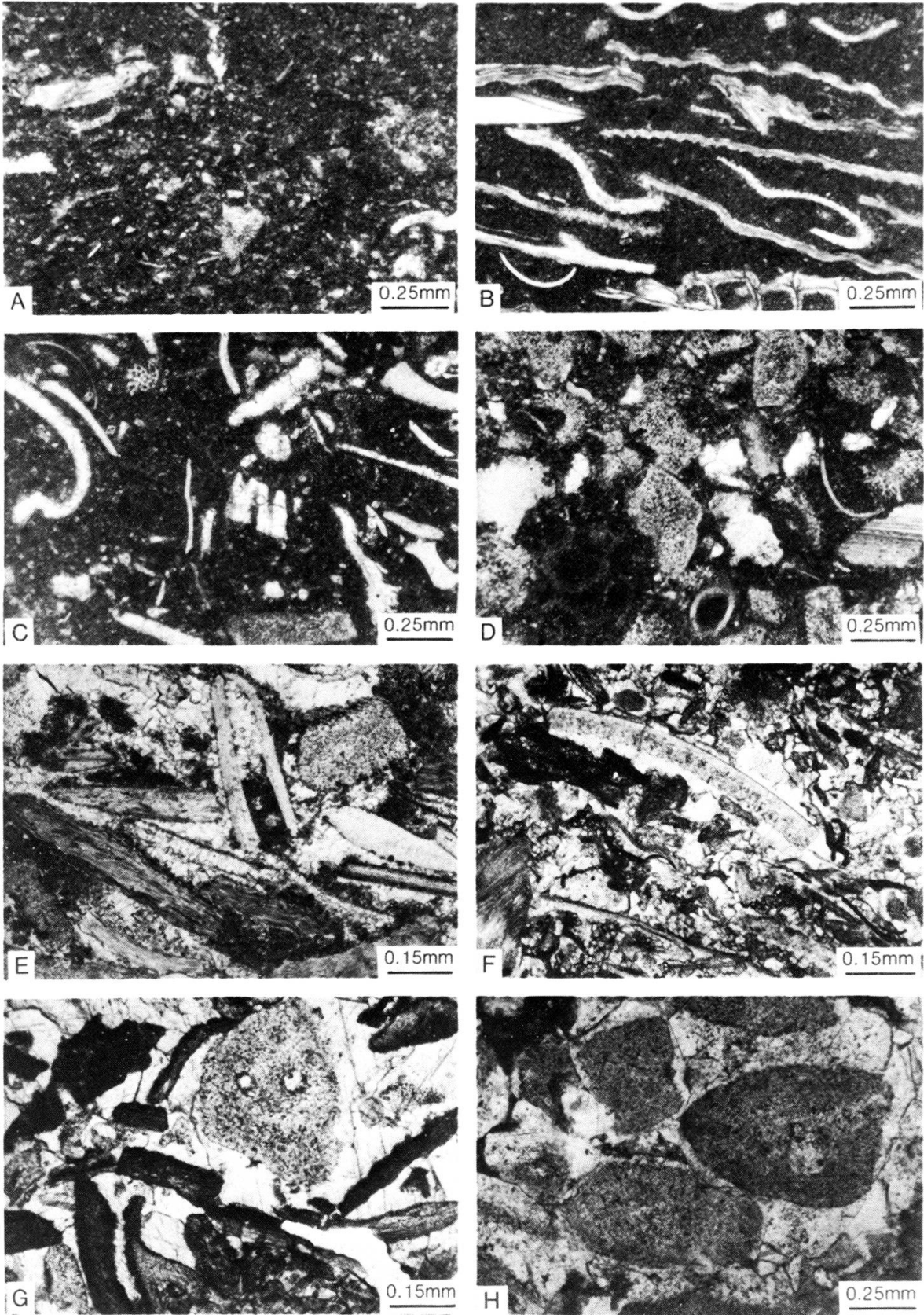


PLATE 1.

Typical microfacies. A. Microfacies 1. B. Microfacies 2. C. Microfacies 3. D. Microfacies 4. E. and F. Microfacies 5. G. Microfacies 6. H. Microfacies 7. See text for detailed descriptions. All photomicrographs: plane polarized light.

PLATE 2.

Typical tempestite (microfacies 5). Moderately bioturbated and disorganized grain-supported biocalcirudite with sparite cement and calcisiltite matrix. Brachiopods and pelecypods predominate over gastropods, bryozoans, crinoids, and trilobites. The bioclasts display an irregular texture where the fine to medium components are concentrated in lower half of photomicrograph with calcite cement (at lower right corner) and calcisiltite matrix (at lower left corner). Larger shells of brachiopods and pelecypods are in equilibrium position at top of photomicrograph with calcite cement and rare calcisiltite matrix. Note dissolution feature in large cavity with typical geopetal internal sediment overlain by sparite cement (arrow). Plane polarized light.



PLATE 3.

Typical tempestite (microfacies 5). Moderately bioturbated and disorganized grain-supported biocalcirudite with sparite cement and pelletoidal calcisiltite matrix. Brachiopods and pelecypods predominate over gastropods, crinoids, phosphatic trilobites, and bryozoans. Bioclasts show various orientations either perpendicular, inclined at various angles, or parallel to bedding. Note the surface of mud at bottom and geopetal internal sediment overlain by sparite cement under brachiopod shells (middle left and bottom).

Burrows are partially filled with sparite cement and calcisiltite matrix. Plane polarized light.



PLATE 4.

Typical tempestite (microfacies 6). Bioturbated grain-supported biocalcarene with sparite cement and rare calcisiltite matrix. Brachiopod and crinoid fragments predominate over trilobites, pelecypods, bryozoans, and ostracods. Note reworking features: breakage, imbrication, random orientation of large shell fragments, and incipient graded bedding of bioclasts. The calcisiltite matrix is mostly at the bottom and the sparite cement at middle and top. Plane polarized light.



PLATE 5.

Typical tempestite (microfacies 6). Moderately bioturbated grain-supported biocalcarenite with sparite cement and calcisiltite matrix. Crinoids and gastropods predominate over brachiopods, ostracods, trilobites, bryozoans, and neomorphosed pelecypod fragments. Other components are lithic pellets and calcisiltite intraclasts. Note incipient graded bedding, concave upward fragments of pelecypod shells, and sharp erosional contact with underlying microfacies 1. The calcisiltite matrix is concentrated at top and the sparite cement is at middle and bottom. Plane polarized light.

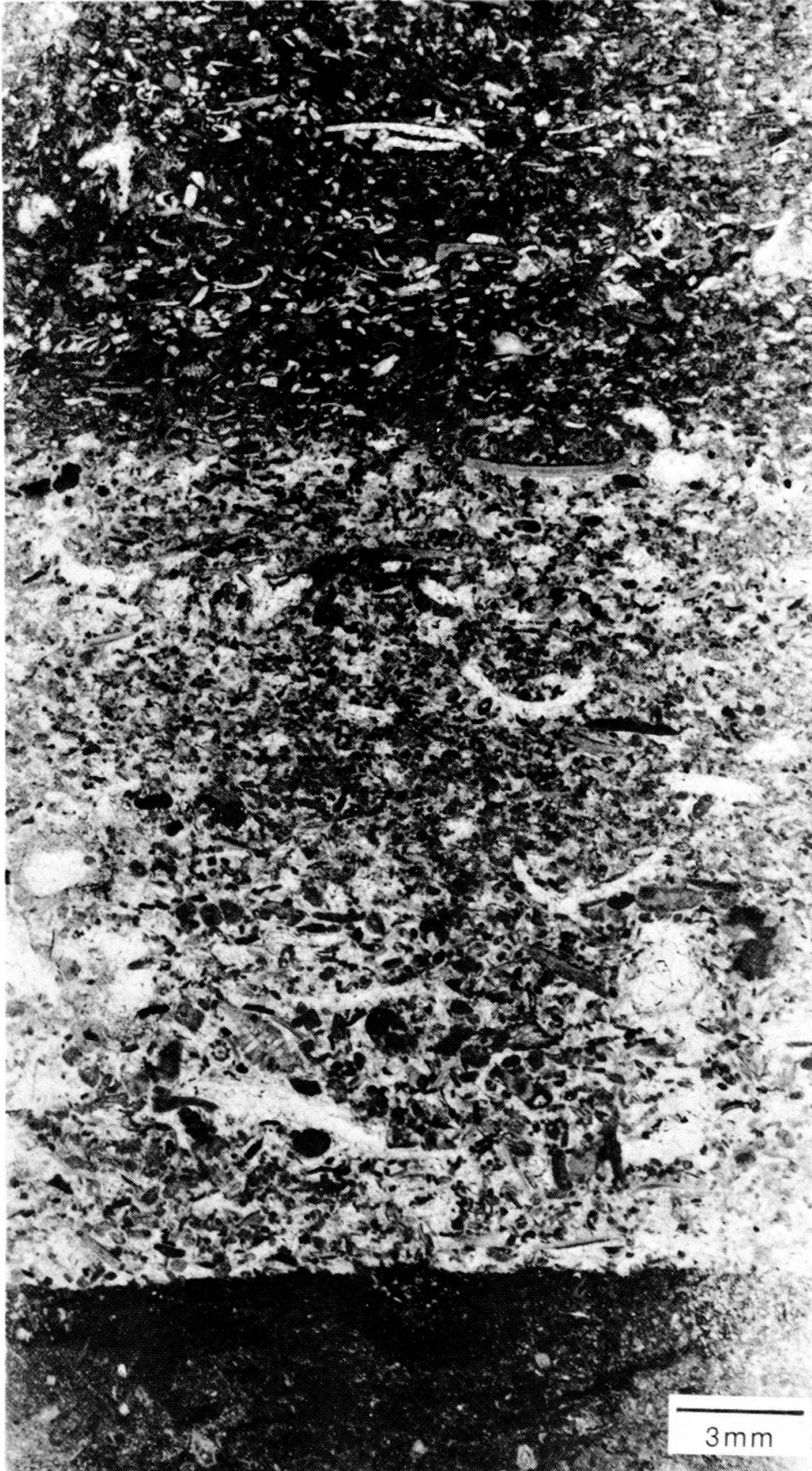


PLATE 6.

Diagenetic sequence. *Marine phreatic environment*. A. Horizontal burrow in calcisiltite partially and selectively replaced by dolomite rhombs. B. Smooth hardground between grain-supported biocalcarenite and overlying calcisiltite. Notice iron oxides concentrated in crust of hardground and decreasing in importance downward, and microfault infilled with sparite cement. C. Irregular hardground surface between grain-supported biocalcarenite with calcisiltite matrix and overlying grain-supported to pressure-welded biocalcarenite with sparite cement. Notice gastropod shell truncated by hardground surface. D. Thin isopachous rim cement around trilobite surrounded by equant sparite cement. Notice small scalenohedral calcite crystals of the rim cement due to its stabilization in the freshwater phreatic environment.

Saturated freshwater phreatic environment. E. Second generation of cavity filling sparite cement nucleated on thin isopachous rim cement itself stabilized in the form of scalenohedral bladed calcite crystals. The cement grades from small to large bladed to large equant mosaic (nicols crossed). F. Aggrading neomorphism from pseudomicrosparite to pseudosparite with elongated loafish crystals in mud-supported biocalcarenite with argillaceous micrite groundmass between crystals. G. Pseudosparite in bioaccumulated limestone. Notice relatively uniform crystal size and argillaceous micrite groundmass between crystals. *Mixing marine freshwater phreatic environment*. H. Silicification after dolomitization where silica replaces dolomite crystals. Note marginal replacement of dark dolomite rhombs (nicols crossed). All photomicrographs: plane polarized light, except E and H nicols crossed.

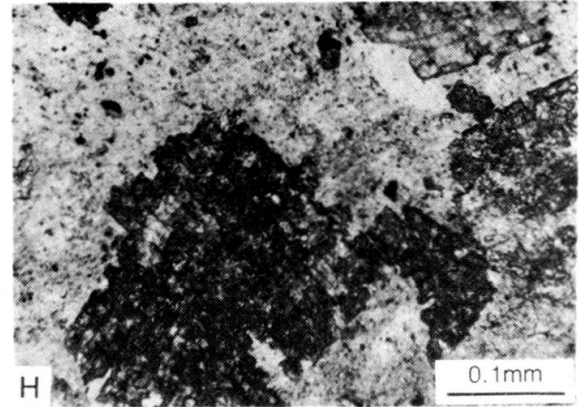
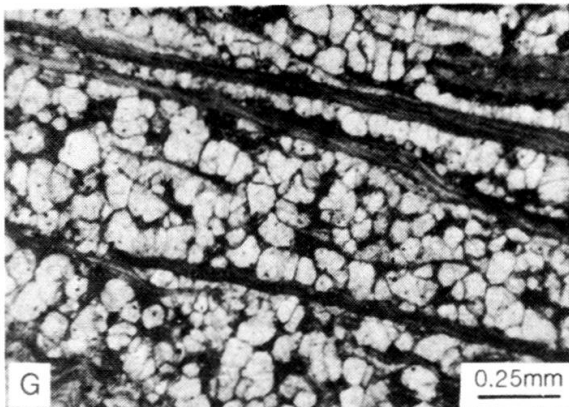
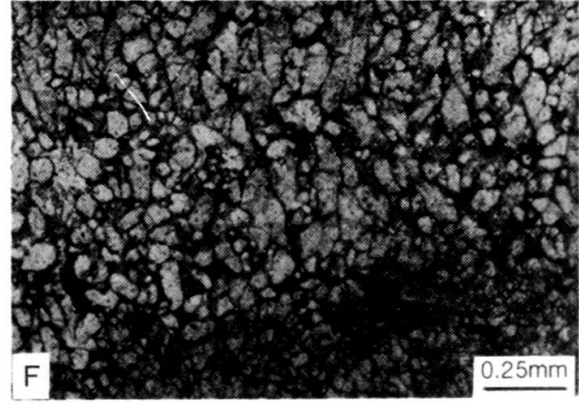
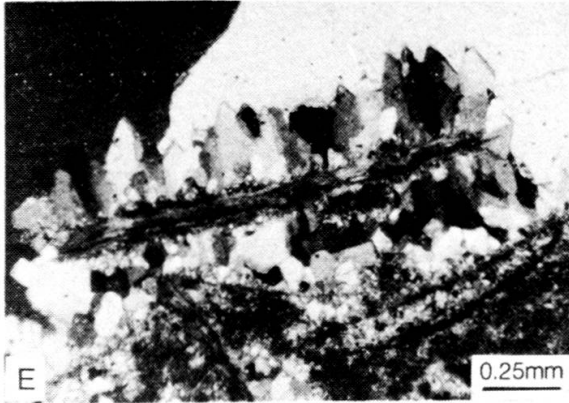
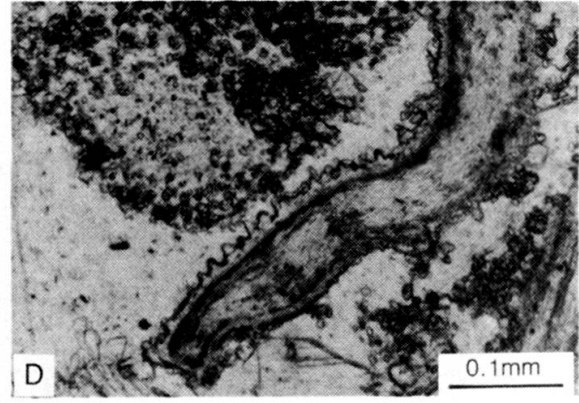
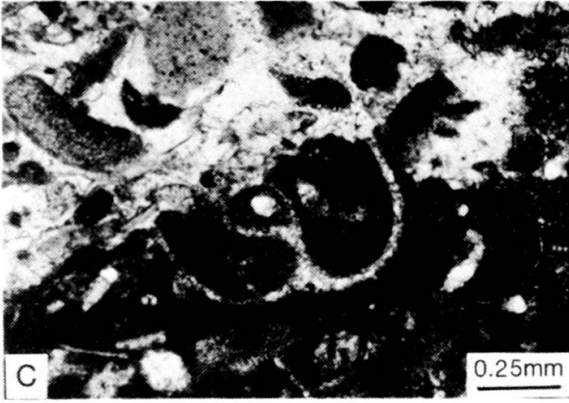
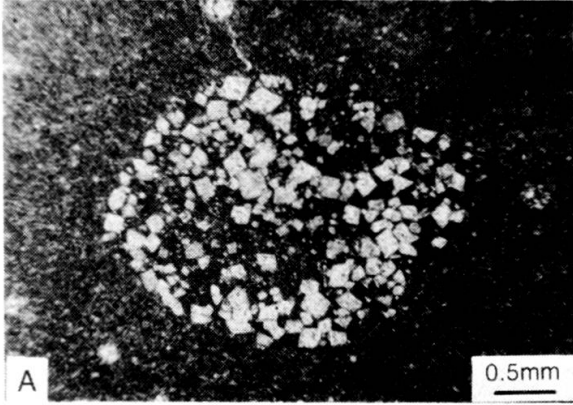


PLATE 7.

Diagenetic sequence (continued). *Marine phreatic environment and storm effects.* A and B. Field photograph and sketch showing three ellipsoidal chert nodules with different orientations in brecciated crinoidal calcisiltite. C. and D. Field photograph and sketch showing three large chert nodules with different orientations in brecciated crinoidal calcisiltite. E. and F. Field photograph and sketch showing partially fragmented elongated chert nodule (center right) and elongated chert nodule fragment (arrow) in vertical position. G and H. Field photograph and sketch showing chert nodule shattered into minute polyhedral fragments (arrow) and large chert nodule (right) broken vertically into two halves with penetration of country rock between fragments. All illustrations from outcrop on Highway 9, Decorah, Iowa.

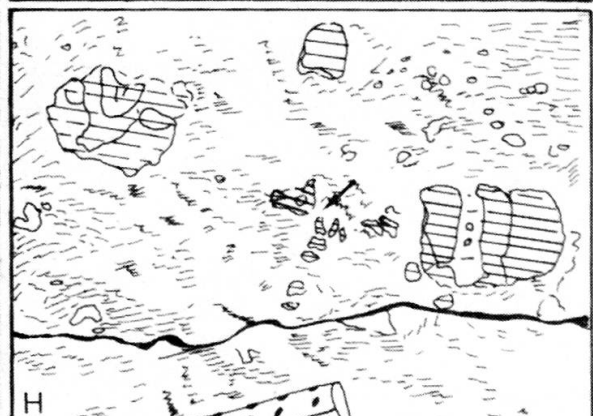
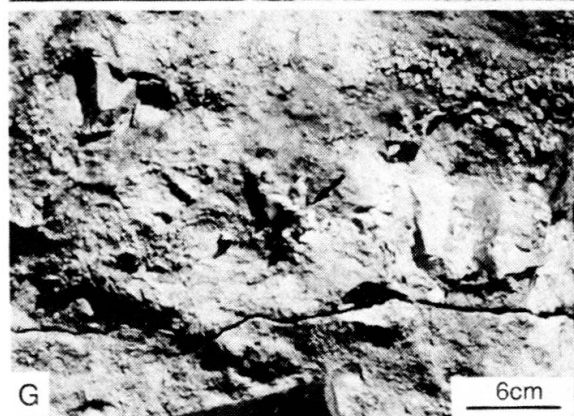
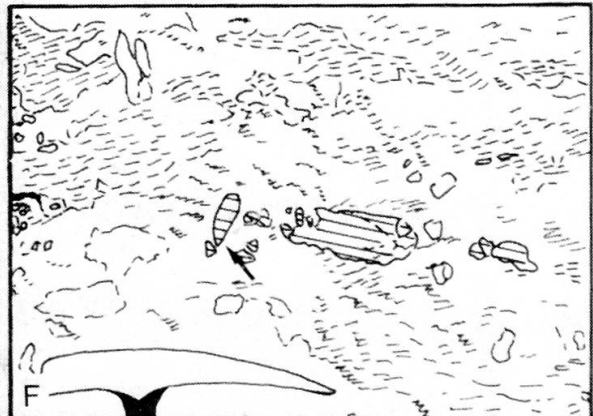
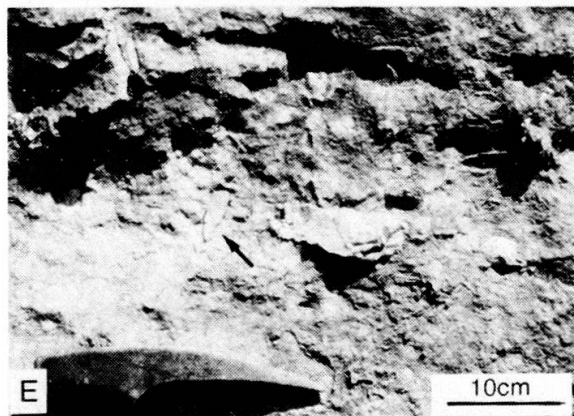
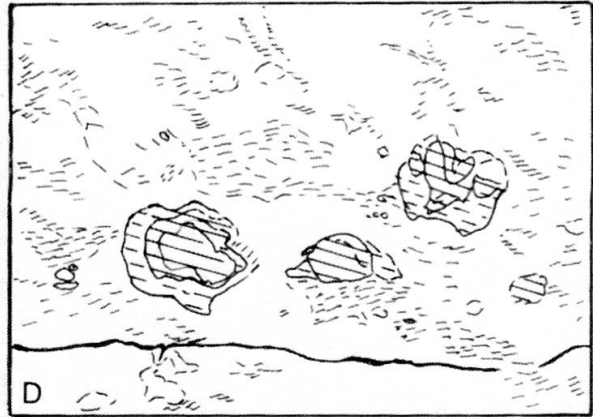
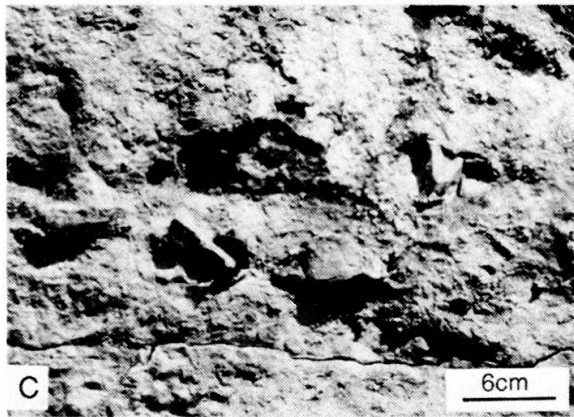
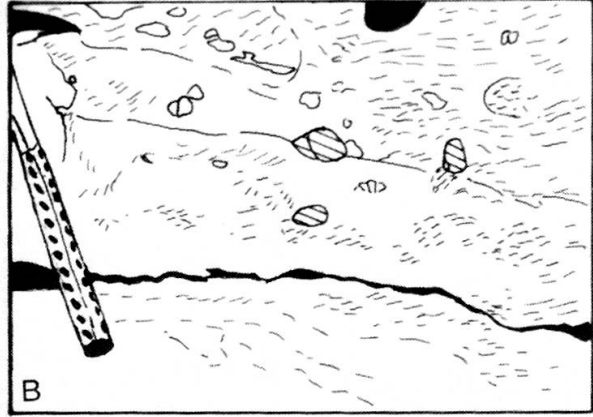
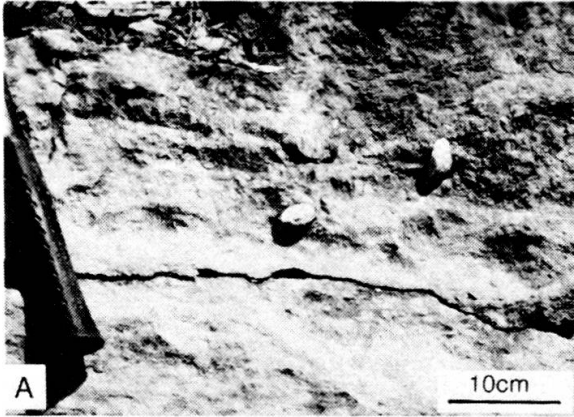


PLATE 8.

Diagenetic sequence (continued). *Mixing marine freshwater phreatic environment*. A. Diagenetic quartz (clear crystal) replacing dolomite rhombs. Iron oxide inclusions within the dolomite survived silicification. *Saturated freshwater phreatic environment II*. B. Poikilotopic calcite cement following in time fabric selective dedolomitization in which dolomite rhombs “float” in calcite and are infilled with dark iron-rich calcite. *Burial environment*. C. Late compaction causing crushing and interpenetration of brachiopod shell fragment by crinoid columnals. D. Sutured stylolite with bituminous residue. E. Pyrite replacing equant sparite cement filling large void in mud-supported biocalcarenite. F. Pyrite infilling secondary porosity after dissolution of dolomite rhombs. Note severe marginal dissolution of dolomite rhombs and their “floating” texture within pyrite. G. Late burial fracturation in mud-supported biocalcarenite. The vertical fracture is infilled with a first generation of scalenohedral calcite directly on the walls and a second generation of coarser sparite in the center. H. Late burial vertical fracture infilled by calcite cement (appearing gray after staining) in dolomitized calcisiltite to mud-supported biocalcarenite. The fracture cuts pyrite seams which replaced dolomite. All photomicrographs: plane polarized light.

